Available online at www.sciencedirect.com
SCIENCE DIRECT®
Journal of the European Ceramic Society 25 (2005) 3469–3477
www.elsevier.com/locate/jeurceramsoc

A structural investigation of the influence of dopants on the electronic properties of $LiCoVO_4$

N. Van Landschoot[a,*], C. Kwakernaak[b], W.G. Sloof[b], E.M. Kelder[a], J. Schoonman[a]

[a] *Laboratory for Inorganic Chemistry, Delft Institute for Sustainable Energy, Delft University of Technology, Julianalaan 136, 2628 BL Delft, The Netherlands*
[b] *Laboratory of Material Science, Delft University of Technology, Rotterdamseweg 137, 2628 AL Delft, The Netherlands*

Received 26 May 2004; received in revised form 10 August 2004; accepted 27 August 2004

Abstract

The influence of 6% Co substitution in $LiCoVO_4$ for Fe, Cr and Cu was investigated to determine the influence on the structural and electronic properties of the substituted inverse spinel. It was found that the lattice parameter of the inverse spinel structure changed and that no second phases were found. The oxidation state of the different ions were determined by XPS and it was found that for both the Fe^{3+} and Cr^{3+} substitution the oxidation state of the Co^{2+} did not change. The XPS results showed that the oxidation state of vanadium was 5+ and is the only cation that partly changed to an oxidation state of 4+, for charge compensation. This change in the oxidation state led to an increase in the electrical conductivity by a factor of 10. The Cu^{2+} substitution also led to an increase in the electrical conductivity but smaller. Rietveld refinement analyses of the inverse spinel led to the conclusion that no large reorientation occurred for the different cations at the different sites.

Keywords: Electrical conductivity; Batteries; X-ray methods; Inverse spinel; $LiCoVO_4$

1. Introduction

The rapid development of modern electronic technology creates a strong demand for portable power sources. Lithium batteries are considered to be the best choice, as they provide high output power and moderate lifetime. The limiting factor in the capacity is the cathode material. In this respect, much effort has been made to improve the performance of the electrode materials. Electrode materials are based on the redox potential difference of the electrode in the course of intercalation/deintercalation reactions.[1] They are generally well-crystalline host compounds either with layered structure such as graphite,[2] $LiCoO_2$[3] and $LiNiO_2$,[4] or with tunnel structure like $LiMn_2O_4$.[5] Generally, compounds with a three-dimensional framework are more stable than two-dimensional compounds.[1] Lithium ion diffusion is clearly easier in a three-dimensional framework than in a two-dimensional framework, because in the former structure the number of contact points of the diffusion paths for lithium ions is larger than that in the latter. The spinel phase materials are of extreme interest as the cathode active materials for their high energy density. Most of the high voltage (>4.5 V) cathodes have the spinel structure with the general formula $Li_{1-x}Mn_{2-y}M_yO_4$ (M = Cr, Fe, Co, Ni, and Cu)[6–14] or the inverse spinel $LiMVO_4$ (M = Ni, Co).[15] The charge and discharge voltage in the 5 V region depend on the transition metal ion M and the amount of cation substitution in $Li_{1-x}Mn_{2-y}M_yO_4$. As a result, the high voltage (>4.5 V) capacity of these manganese-based $Li_{1-x}Mn_{2-y}M_yO_4$ cathodes has generally been attributed to the other transition metal ion redox couples such as $Fe^{3+/4+}$, $Ni^{2+/3+/4+}$, $Cu^{2+/3+}$.

The inverse spinel material, $LiCoVO_4$, has not been studied intensively, despite the high theoretical capacity of 148 mAh/g. Van Landschoot et al.[16] showed that the use

* Corresponding author.
E-mail address: N.VanLandschoot@TNW.TUDelft.nl (N.V. Landschoot).

0955-2219/$ – see front matter © 2004 Elsevier Ltd. All rights reserved.
doi:10.1016/j.jeurceramsoc.2004.09.006

of certain dopants (Fe, Cr and Cu) improves the electrical conductivity and increases the cycle efficiency of $LiCoVO_4$. From a structural point of view it was still unclear what caused the increase in the electronic conductivity. In this paper we partly substituted 6 mol% Co in $LiCoVO_4$ for either Fe, Cr and Cu. The structural parameters have been examined by X-ray diffraction (XRD) and fitted using Rietveld refinement. X-ray photoelectron spectroscopy (XPS) is used to determine the influence of the dopants on the oxidation state of the cations and electrochemical impedance spectroscopy (EIS) was used to investigate the electronic parameters.

2. Experimental

$LiCo_{0.94}M_{0.06}VO_4$ (M = Co, Cu, Cr, and Fe) was prepared via a citric acid complex method.[16] Appropriate amounts of Li_2CO_3 (Baker Analyzed, >99%), $CoCO_3{\cdot}H_2O$ (Merck, >99%), NH_4VO_3 (Acros Organics, >98%) were mixed together in 100 ml of distilled water under constant magnetic stirring at 80 °C. As dopants, $C_4H_6CuO_4{\cdot}H_2O$ (Riedel de Haen, >99%), $FeCl_2{\cdot}4H_2O$ (Acros Organics, >98%), and $Cr_3(OH)_2(CO_2CH_3)_7$ (Acros Organics, >98%) were used. To the solution 100 ml of a 0.3 molar citric acid solution was slowly added to the dispersion. The solution was then kept at 100 °C for 1 h forming a gel. Subsequently, the gel was heated at 120 °C in a vacuum furnace for 3 h. The obtained precursor was fired at 500 °C in air for 2 h with intermediate ball milling.

X-ray diffraction was used to determine the phase purity and structural parameters of the powdered materials with a Bruker D8 Advance X-ray diffractometer with Cu Kα radiation. The X-ray powder diffraction patterns were collected at a step size of 0.007° with a step time of 5 s in a range of 15–140° in 2θ. The single-phase spectra were refined using Topas R,[17] a Rietveld refinement program, to obtain the structural parameters.

On the powdered samples XPS measurements were performed with a PHI 5400 ESCA equipped with a dual Mg/Al anode X-ray source, a spherical capacitor analyser (SCA), and a 5 keV ion-gun. The sample surface was tilted 30° with respect to the optical axis of the input lens of the electron analyser. The input lens aperture used was 3.5 mm × 1.0 mm. The spectra were recorded using non-monochromatic Mg Kα (1253.6 eV) or Al Kα (1486.3 eV) radiation. The X-ray source was operated at 15 kV and 400 W. The energy scale of the SCA was calibrated according to a procedure described in ref.[18] The instrument was set at constant analyzer pass energy of 44.75 eV recording a survey spectrum from 0 eV to 1000 eV binding energy (BE) with a step size of 0.25 eV. The individual photoelectron spectra were measured using a step size of 0.2 eV. The spectra were corrected for the non-monochromatic nature of the X-ray source[19] and also for the kinetic energy (KE) dependent transmission of the spectrometer by multiplying each spectral intensity with its corresponding kinetic energy. Next, the background intensity was subtracted from the spectra using a Shirley method.[20] To exclude any effects on the values of binding energies due to a charging of the sample during the XPS analysis, all data are corrected by a linear shift such that the peak maximum of the C1s binding energy of adventitious carbon corresponds with 284.80 eV. Then the spectra were fitted with symmetrical mixed Gauss–Lorentz functions using a linear least-squares method to resolve the chemical states of the constituting components. The value of the kinetic energy is obtained as follows. The spectrum was first shifted using the C1s peak, and then, the spectra of the Auger line regions were differentiated twice to obtain the minimum which is the position of the auger line maximum was taken at the second derivative.

For the conductivity measurements, the $LiCo_{0.94}M_{0.06}VO_4$ (M = Co, Cu, Cr, and Fe) powders were pressed into pellets with a diameter of 10 mm and an average thickness of 1 mm at a pressure of 1500 kg/cm^2. The pellets were then sintered at 500 °C for 16 h in air. After the sintering step, the pellet surfaces were sputtered with gold for 10 min on both sides using a sputter coater (Edwards). The electrical conductivity measurements were performed using a Schlumberger Solatron 1260 Frequency Response analyser. The applied ac voltage was 10 mV peak-peak in the frequency range 1–10 MHz. The temperature range was between 50 °C and 160 °C. The obtained spectra were fitted afterwards using Zview 2.[21]

3. Results and discussion

The X-ray diffraction patterns for the 6 mol% substituted $LiCoVO_4$ could be assigned to a cubic symmetry and it was fitted by the Rietveld refinement method. All the observed reflections could be indexed in the space group *Fd*3*m* (No. 227) in which all cations were distributed on the tetrahedral (8a) and octahedral (16d) sites. The structural fitted parameters for the pure and substituted $LiCoVO_4$ are reported in Table 1. Fig. 1 shows the Rietveld refinement of the XRD patterns. The refined XRD patterns showed no impurities, indicating that the materials were phase pure. The refined patterns all showed good fit parameters as seen in Table 1. The inverse spinels were very difficult to fit due to the inverse structure. To simplify the fitting procedures boundary conditions were used and these are also listed in Table 1.

The refinement results showed that the dopants are located on the octahedral site, which was expected for Cr and Fe because they have a tendency to occupy octahedral positions.[24,25] The refinement of the Cu-substituted material show that the Cu ions also occupy the octahedral position, although, the Cu ions also have the tendency to occupy the tetrahedral sites.[26] To rule out the possibility of any dopants at the tetrahedral sites, neutron diffraction measurements have been performed at ISIS and these results will be published in a forthcoming article. The Fe substituted spinel shows a decrease of the lattice parameter when compared to $LiCoVO_4$, indicating that the ionic radius of the dopant is most likely smaller than that of the Co^{2+} (0.75 Å) ion. Thus, the dopant

Table 1
Crystallographic data, including lattice parameters, site occupancy for $LiM_{0.06}Co_{0.94}VO_4$ (M = Fe, Cr, and Cu) determined via the Rietveld analysis

Sample	$LiCoVO_4$	$LiFe_{0.06}Co_{0.94}VO_4$	$LiCr_{0.06}Co_{0.94}VO_4$	$LiCu_{0.06}Co_{0.94}VO_4$
Space group	*Fd*-3*m* [O_h^7]	*Fd*-3*m* [O_h^7]	*Fd*-3*m* [O_h^7]	*Fd*-3*m* [O_h^7]
a (Å)	8.281	8.278	8.275	8.285
Volume (Å^3)	567.87	567.25	566.63	568.69
Site occupancy				
Li_{16d}	0.98	0.99	0.95	0.96
Co_{16d}	0.97	0.86	0.82	0.89
V_{16d}	0.05	0.07	0.10	0.07
M_{16d}	–	0.06	0.06	0.06
Li_{8a}	0.01	–	0.05	0.02
Co_{8a}	0.04	0.07	0.04	0.05
M_{8a}	–	–	–	–
V_{8a}	0.95	0.93	0.90	0.93
O_{32e}	1.00	1.00	1.00	1.0
R_{wp}; R_{bragg}	5.36; 7.59	4.34; 4.05	2.58; 3.65	2.88; 3.15
Formula obtained	$Li_{0.98}Co_{0.97}V_{0.05}$	$Li_{0.99}Fe_{0.06}Co_{0.86}V_{0.07}$	$Li_{0.95}Cr_{0.06}Co_{0.82}V_{0.10}$	$Li_{0.96}Cu_{0.06}Co_{0.89}V_{0.07}$
	$[Li_{0.01}Co_{0.04}V_{0.95}]O_4$	$[Co_{0.07}V_{0.93}]O_4$	$[Li_{0.05}Co_{0.04}V_{0.90}]O_4$	$[Li_{0.02}Co_{0.05}V_{0.93}]O_4$

Strains: $Co_{16d} = 2 - Li_{16d} - V_{16d} - M_{16d}$, $V_{8a} = 1 - V_{16d}$.

ions must have an oxidation state of Fe^{3+} and an ionic radius of 0.645 Å. The lattice parameter of the Cu-doped samples increased indicating that the ionic radius of the dopant ion is larger than Co^{2+} −0.91 Å and 0.86 Å for the Cu^+ and Cu^{2+} ions, respectively. The lattice parameter of the Cr-doped material decreases possibly indicating a Cr^{3+} valence state. The valence state of the dopant ions should have an effect on the valence states of the other 3d metals, which was further investigated using XPS.

The obtained cell parameter for $LiCoVO_4$ (8.281 Å) for this sample is consistent with reported data[15] and the lattice parameters for the substituted spinels are 8.278 Å, 8.275 Å, and 8.285 Å for the Fe, Cr and Cu-substituted spinels, respectively. The lattice parameter is an important parameter as it influences the 3d pathway of a Li ion in these inverse spinels. The Li-ion pathway through the inverse spinel is via the 16d–8b–16d sites. The lattice distance between the 16d site and the vacant 8b or 48f site is $(\sqrt{3}/8)a$[22] with a being the lattice parameter. The reduced lattice parameter for the Cr and Fe-substituted inverse spinel should give an increase in the ionic conductivity and should lower the activation energy. Using the same argument for the Cu-substituted inverse spinel an decrease is expected based on the increased lattice parameter.

Fig. 2 shows the XPS photoelectron spectra of the (a) $Fe2p_{3/2}$, (b) $Cr2p_{3/2}$, and (c) $Cu2p_{3/2}$ photoelectron lines for the substituted inverse spinels. These results have been measured using the Mg anode. The values for the binding energy, kinetic energy, and modified Auger parameter (AP) are summarized in Table 2. The solid lines in the figures are the fitted curves of the different XPS spectra. The measured BE value of the $Fe2p_{3/2}$ photoelectrons is 711.17 eV and the corresponding shake-up satellite at 719.19 eV, showing, that Fe is tri-valent in agreement with reported values in the NIST Tables[23] (approximately 711 eV (Fe^{3+}) and 709 eV (Fe^{2+}). This slightly higher BE value was also observed in Fe-substituted $LiFe_{0.5}Mn_{1.5}O_4$ by Amine et al.[27] Tri-valent Fe ions also possess a shake-up structure. The tri-valent state is also in good agreement with the change in the lattice parameter as observed with the Rietveld refinement analyses. The tri-valent state is also confirmed by Mössbauer spectroscopy and will be discussed in a forthcoming article. The BE value of $Cr2p_{3/2}$ of 576.8 eV and the AP value of 1104.6 eV indicate that Cr is tri-valent (approximately 577 eV for Cr^{3+} and 579 eV for Cr^{6+}.[23] This tri-valent nature is in good agreement with the lattice parameter as calculated. The BE value of Cu is 934.5 eV and the shake-up structure, as shown in Fig. 2c, both show that Cu is di-valent.[22] It is observed that only during the XPS measurement the line shape changes due to the X-ray bombardment of Cu^{2+} to Cu^+, adding two 2p-peaks with no satellite structure as shown in Fig. 2c. This phenomenon has also been observed by Fleisch et al.[28] The binding energies in the case of $LiCo_{0.94}Cu_{0.06}VO_4$ are about 0.5 eV lower than for the other dopant and the original substance. This observation can be reproduced every measurement.

Table 2
The binding energy (BE), kinetic energy (KE) and modified Auger parameters (AP) for the dopants of the substituted inverse spinel materials

Sample	$2p_{3/2}$ (eV)	$2p_{1/2}$ (eV)	LMM (eV)	AP (eV)	$2p_{3/2}$ shake up	$2p_{1/2}$ shake up
$LiCr_{0.06}Co_{0.94}VO_4$	576.79	586.18	725.77	1104.62	–	–
$LiFe_{0.06}Co_{0.94}VO_4$	711.97	724.59	554.25	1411.32	718.80	–
$LiCu_{0.06}Co_{0.94}VO_4$ (Cu^{2+})	934.49	952.31	337.32	1850.77	942.25	962.13
$LiCu_{0.06}Co_{0.94}VO_4$ (Cu^+)	932.39	952.31	337.32	1848.69	–	–

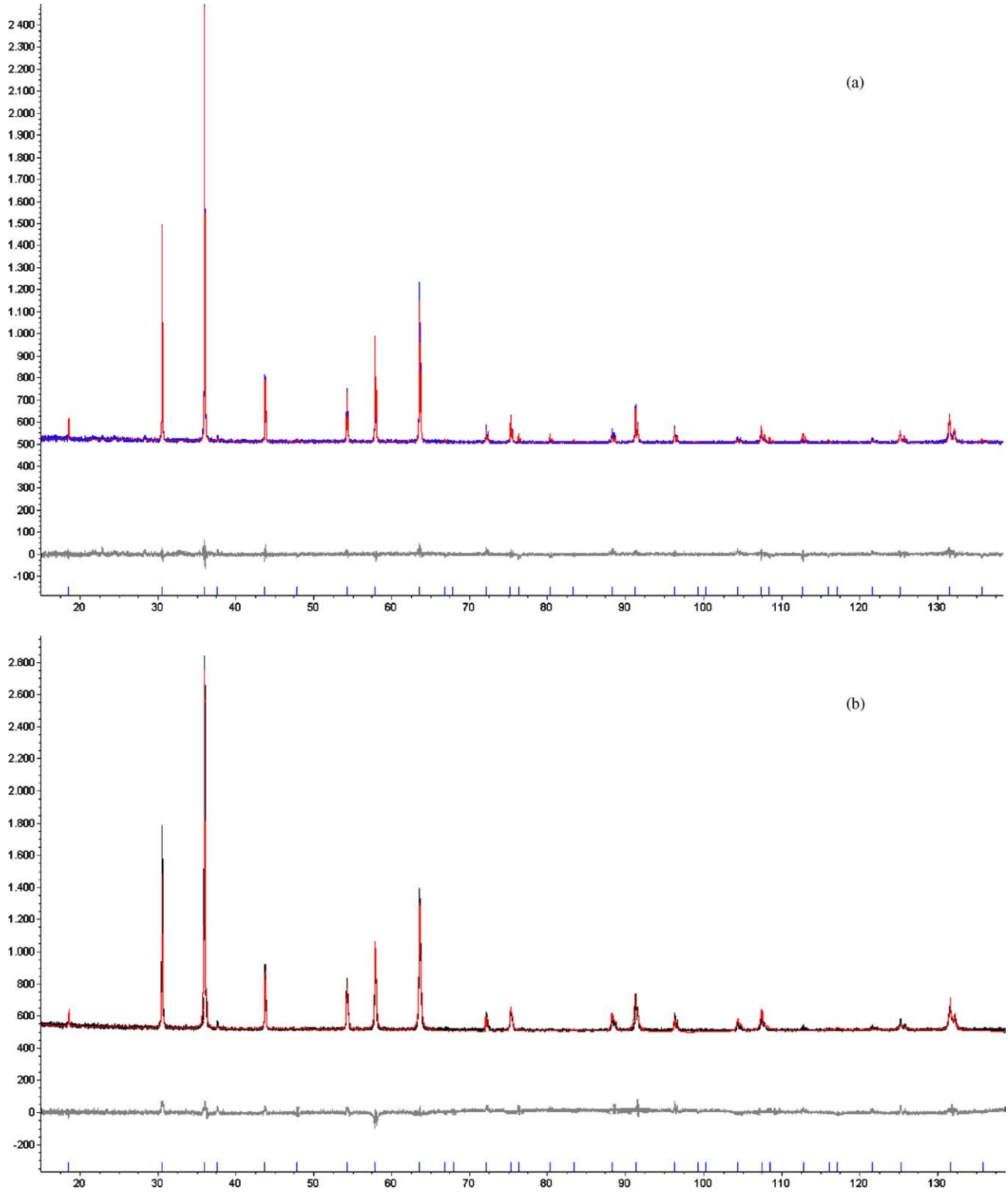

Fig. 1. X-ray diffractograms for: (a) $LiCoVO_4$; (b) $LiFe_{0.06}Co_{0.94}VO_4$; (c) $LiCr_{0.06}Co_{0.94}VO_4$; (d) $LiCu_{0.06}Co_{0.94}VO_4$. The lines in the diffractograms are calculated by the Rietveld analysis. The differences between the calculated and the observed patterns are represented below the corresponding diffractograms. The vertical bars represent the positions of the diffraction peaks.

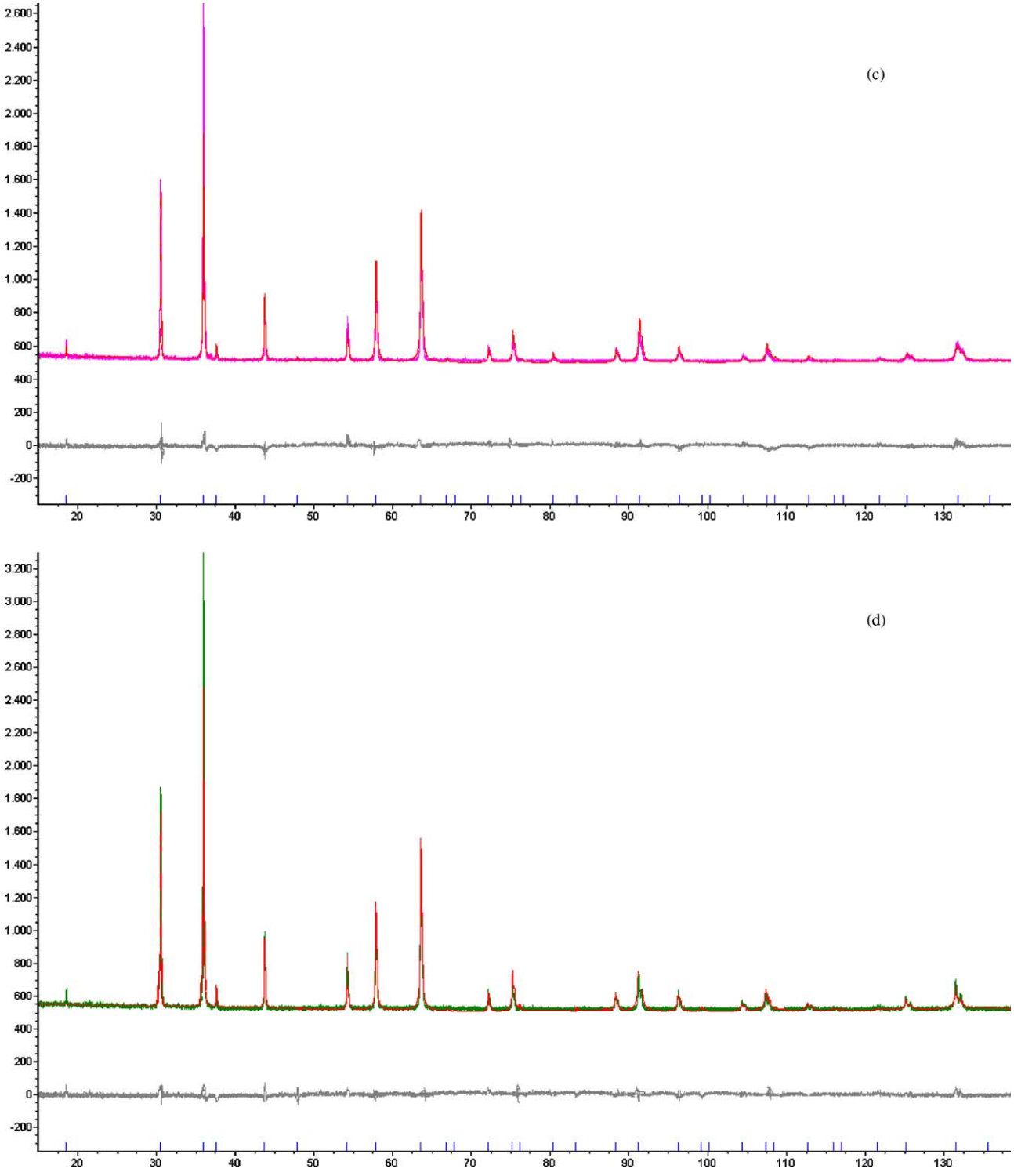

Fig. 1. (*Continued*).

Fig. 3 shows the XPS emission of the Co2p lines (a) and Auger LMM lines (b) of the pure and substituted spinels. These results were measured using the Mg anode at 400 W and corrected for charging with the C1s energy of 284.80 eV as a reference value. The values for the binding energy, kinetic energy and modified Auger parameter of Co ions are summarized in Table 3. The shake-up lines point unambiguously to Co^{2+} and the BE of $Co^{2+}(2p_{3/2})$ is 780.4+/−0.3 eV (according to several values presented by NIST).[23] The dopants have no influence on the valence state of the Co^{2+} ions in the

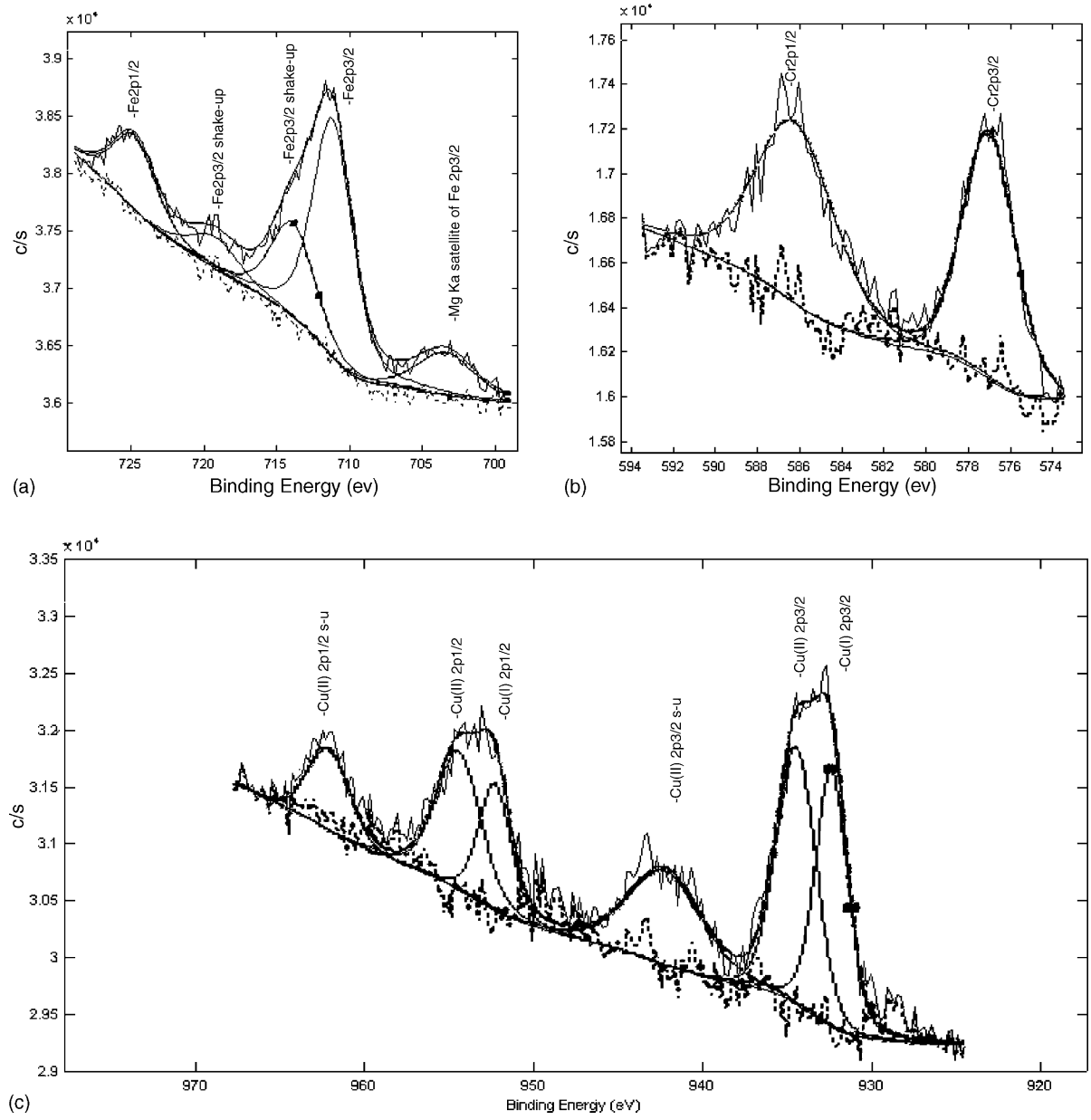

Fig. 2. The structure of the dopants in the substituted inverse spinels for: (a) Fe2p lines, (b) Cr2p lines, and (c) the Cu2p lines. The chemical shift is the indication that Fe ions are trivalent. The shake-up satellite of the $Fe2p_{3/2}$ peak belongs to Fe^{3+} ions. The shake-up satellites are the indicator for Cu^{2+} ions. The Cu^{+} is not a component of the original material but is formed during the XPS measurement due to the reduction of Cu^{2+} to Cu^{+} under X-ray bombardment.

present inverse spinel structure. No traces of mono-valent Co were found for the Fe^{3+} and Cr^{3+} substituted spinel as possible charge compensation. The modified Auger parameter shows little variation so it can be concluded that there is no detectable influence of the dopant ions on the chemical environment of the Co^{2+} ions. This is in agreement with the Rietveld refinement where no substantial reorientation of the cobalt ions took place or a possible phase transition. For

Table 3
The binding energy (BE), kinetic energy (KE), and modified Auger parameters (AP) for cobalt in the inverse spinel materials

Sample	$Co2p_{3/2}$ BE (eV)	$Co2p_{1/2}$ BE (eV)	$Co2p_{3/2}$ shake up	$Co2p_{1/2}$ shake up	Co LMM KE (eV)	Mod. AP ($2p_{3/2}$)
$LiCoVO_4$	780.40	796.52	787.12	803.19	480.49	1553.51
$LiCr_{0.06}Co_{0.94}VO_4$	780.49	796.85	787.40	803.20	480.56	1553.53
$LiFe_{0.06}Co_{0.94}VO_4$	780.66	797.01	787.54	803.47	480.64	1553.62
$LiCu_{0.06}Co_{0.94}VO_4$	780.21	796.44	786.93	803.02	480.18	1553.63

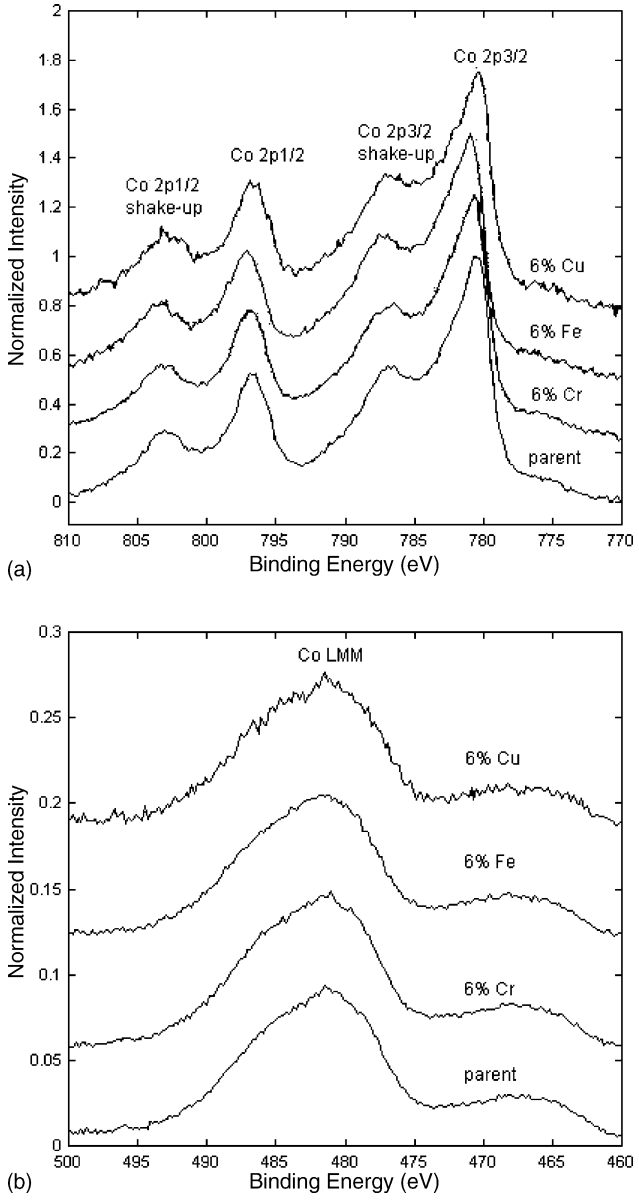

Fig. 3. The line shapes of the cobalt 2p lines (a) and auger LMM lines (b) indicate that there is no chemical change of cobalt (II) ions due to the presence of dopants.

charge compensation, it is very unlikely that the inverse spinel system accepts oxide ion vacancies of more than 3% and, therefore, it is suggested that the vanadium ions change in oxidation state. The values for the binding energy of oxygen and vanadium of the compounds $LiCo_{0.94}X_{0.06}VO_4$ (X = Co, Cu, Cr and Fe) are measured using the Mg anode (as shown in Fig. 4). The measured values for $O2p_{3/2}$ correspond well with those of V_2O_5 and other oxides as shown in Table 4. The lower value for Cu corresponds to CuO. The shape of the V2p lines do not change with the dopant. The BE values of V^{3+}, V^{4+}, and V^{5+} are 512.4 eV, 515.5 eV and 517.4 eV, respectively.[29] The values of the BE of $V2p_{3/2}$ are slightly lower compared tot the BE of V^{5+}. This may indicate the presence of V^{4+} although the width and shape of the $V2p_{3/2}$ peak do not change much as the dopant concentration is too low.

Table 5
The values for the binding energy (BE), kinetic energy (KE), and modified Auger parameter (AP) of oxygen and the binding energy of lithium of the compounds $LiCo_{0.94}X_{0.06}VO_4$ (X = Co, Cr and Fe)

Sample	O1s (eV)	O KVV	Mod. Ap. O1s	Li1s (eV)
$LiCoVO_4$	530.08	974.26	1042.42	54.53
$LiCr_{0.06}Co_{0.94}VO_4$	530.27	974.41	1042.46	54.54
$LiFe_{0.06}Co_{0.94}VO_4$	530.22	974.23	1042.59	54.95

The values for the binding energy, kinetic energy, and modified Auger parameter of oxygen and the binding energy of lithium of the compounds $LiCo_{0.94}X_{0.06}VO_4$ (X = Co, Cr and Fe) are shown in Table 5. These results were measured using the Al anode. The Li^+ BE values for the different substituted spinels are close to the value observed for Li_2O (Fig. 4).[30]

Fig. 5 shows the impedance spectra of the various pellets measured at 160 °C and the equivalent circuit is presented in the spectra. The sample dimensions have been used in the analyses of the measurements. Since $LiCoVO_4$ is a mixed ionic and electronic conductor (MIEC), two parallel branches representing ionic–electronic conduction pathways are expected. The use of Li^+-ion blocking electrodes results in a DC conduction pathway for electrons and blocking behaviour for Li^+-ions under DC conditions.[31] The data can be fitted including a constant-phase element (CPE) with impedance $Z_{CPE} = k(i\omega)^{-\alpha}$ to allow for depression of the arc.

The spectra recorded at higher temperatures revealed excellent fit results ($\chi^2 < 10E{-}5$ for the various powders). The α value for the $LiCoVO_4$ is 0.64 and decreases to 0.61 at 160 °C. The α values for the substituted spinels are slightly higher 0.70 for the Cu-substituted inverse spinel and 0.69 for both Fe and Cr-substituted inverse spinels. Fig. 6 shows Arrhenius plots of the electrical conductivities of the pellets derived from R_{bulk}. The electronic conductivity, obtained from R_{bulk}, for $LiCoVO_4$ is 7×10^{-9} S/cm at 50 °C, this value is also found by Fleisch

Table 4
The binding energy (BE), kinetic energy (KE) for oxygen and vanadium in the inverse spinel materials

Sample	O1s	$V2p_{3/2}$	$V2p_{1/2}$	Difference ($V2p_1 - V2p_3$)	Difference ($O1s - V2p_3$)
$LiCoVO_4$	529.90	516.58	524.22	7.64	13.32
$LiCr_{0.06}Co_{0.94}VO_4$	530.04	516.84	524.17	7.33	13.20
$LiFe_{0.06}Co_{0.94}VO_4$	530.15	516.87	524.26	7.39	13.28
$LiCu_{0.06}Co_{0.94}VO_4$	529.70	516.45	523.88	7.43	13.25

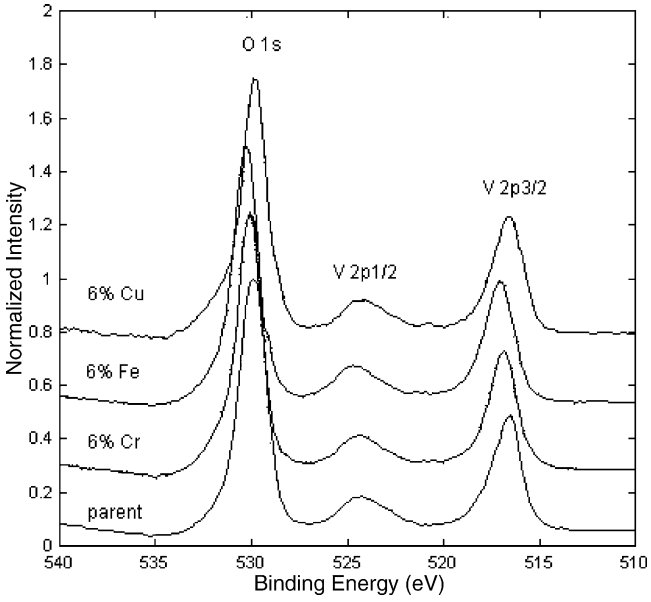

Fig. 4. The line shapes of the vanadium 2p lines and oxygen O1s line show that there is no chemical change as the dopant elements are incorporated in the original material.

et al.[28] The electronic conductivity for the substituted inverse spinels derived from R_{bulk} is for $LiCo_{0.94}Cr_{.06}VO_4$ 10^{-7} S/cm, 4×10^{-8} S/cm for the $LiCo_{0.94}Cu_{0.06}VO_4$ material, and 4×10^{-8} S/cm for $LiCo_{0.94}Fe_{0.06}VO_4$. The activation energies for R_{bulk} are 0.32 ± 0.02 eV for $LiCoVO_4$, 0.22 ± 0.02 eV for $LiCo_{0.94}Cu_{0.06}VO_4$, 0.19 ± 0.02 eV for $LiCo_{0.94}Cr_{0.06}VO_4$, 0.21 ± 0.02 eV for $LiCo_{0.94}Fe_{0.06}VO_4$. For electrode materials conditions for electron transport, especially at low electrical conductivity in the order of 10^{-7} S/cm, is related to small polaron hopping which

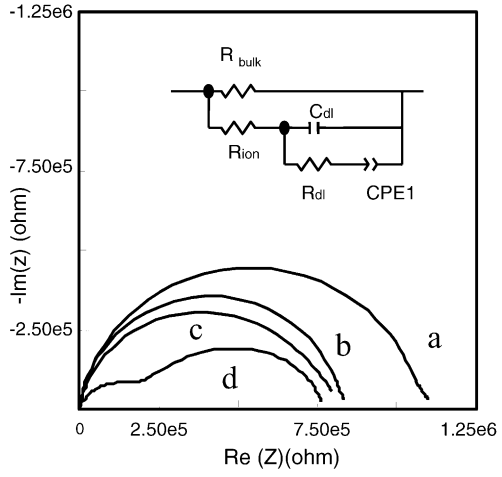

Fig. 5. Impedance spectra of the cells: (a) Au //$LiCoVO_4$// Au, (b) Au //$LiCo_{0.94}Cu_{0.06}VO_4$// Au, (c) Au //$LiCo_{0.94}Fe_{0.06}VO_4$// Au, (d) Au //$LiCo_{0.94}Cr_{0.06}VO_4$// Au, measured at 160 °C between 1 Hz and 10 MHz. The sample geometry and thickness have been taken into account in the analyses of the measurements.

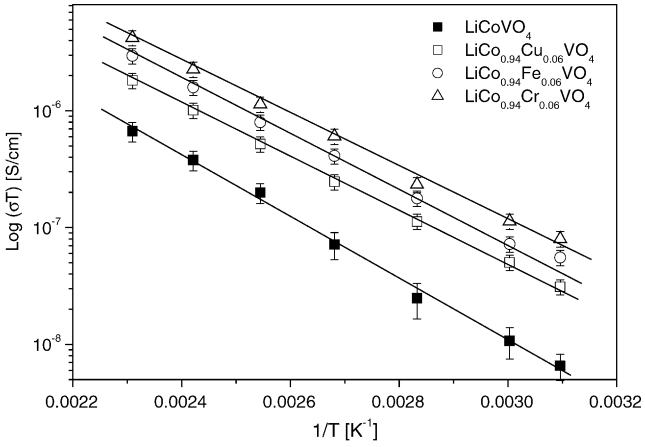

Fig. 6. Electrical conductivities in (S/cm) of the pristine, $LiCoVO_4$, and the substituted inverse spinel, $LiCo_{0.94}M_{0.06}VO_4$ (M = Fe, Cr, Cu), pellets as a function of the reciprocal temperature.

is related to relative high migration activation energies 0.2–0.3 eV.[33,34] In the spinel-type $LiMn_2O_4$ the polaron hopping mechanism is not altered by changes in oxygen non-stochiometry or other chemical deintercalation or by the introduction of different dopants (Cu, Cr, Fe, and Ni). A similar charge transport mechanism is found for the inverse spinel-type $LiCoVO_4$. The charge transport mechanism is not altered by the introduction of the dopants. The decrease in the activation energy of the substituted inverse spinels indicates that the carrier mobility increases upon substitution. The Fe^{3+} ($3d^5$) and Cr^{3+} ($3d^3$) substitution for Co^{2+} ($3d^7$) lowers the valence state of the V^{5+} ($3d^0$) to V^{4+} ($3d^1$) but increases the carrier mobility. The lattice parameter of these materials also decreases which benefits the electronic transport. For the Cu^{2+} ($3d^9$) substitution the valence state of the V^{5+} ion does not change but the electronic activation energy does decrease and the lattice parameter of the Cu-doped $LiCoVO_4$ increases. The position of the 3d states of Cu is below the 3d states of Co.[33] This lowers the Fermi level of the material, as seen by the XPS results where the BE values of the Cu-doped $LiCoVO_4$ is 0.5 eV lower compared to the other materials. The lowering of the Fermi level enhances the charge transport. The lowering of the Fermi level has a beneficiary effect on the potential of the material during charging. This increase in the potential is observed and reported previously by Van Landschoot et al.[16]

4. Conclusions

A structural investigation of the influence of dopants on the electronic conductivity on $LiCoVO_4$ was done. As dopants 6 mol% Co was substituted for Cu, Cr and Fe. The materials were prepared using a citric-acid assisted synthesis and were phase pure as seen from the XRD patterns. The Rietveld refinement showed that all the different dopants were located on the octahedral sites and that no large reorientation of the

different cations occurred. The XPS results showed that both Fe and Cr had an oxidation state of 3+ and Cu had an oxidation state of 2+. The Co^{2+} cations did not change in oxidation state and it was assumed that the V^{5+} cations reduced partly to V^{4+}, but this was not corroborated by XPS measurements, due to the fact that the BE-values of V^{5+} and V^{4+} are quite similar.

References

1. Wakihara, M. and Yamamoto, O., *Lithium ion Batteries Fundamentals and Performance*. Wiley-VCH, 1998.
2. Huang, H., *Anode Materials for Lithium-ion Batteries*. Ph.D Thesis, Delft University of Technology, 1999.
3. Mizushima, K., Jones, P. C., Wiseman, P. J. and Goodenough, J. B., *Mater. Res. Bull.*, 1980, **15**(6), 783.
4. Dahn, J. R., Von Sacken, U., Juzkow, M. W. and Al-Janaby, H., *J. Electrochem. Soc.*, 1991, **138**(8), 2207.
5. Thackeray, M. M., De Picciotto, L. A., De Kock, A., Johnson, P. J., Nicholas, V. A. and Adendorff, K. T., *J. Power Sources*, 1987, **21**(1), 1.
6. Obrovac, M. M., Gao, Y. and Dahn, J. R., *Phys. Rev. B*, 1998, **57**, 5728.
7. Sigala, C., Guyomard, D., Verbaere, A., Diffard, Y. and Tournoux, M., *Solid State Ionics*, 1995, **81**, 167.
8. Kawai, H., Nagata, M., Tabuchi, M., Tukamoto, H. and West, A. R., *Chem. Mater.*, 1998, **10**, 3266.
9. Shigemura, H., Sakaebe, H., Kageyama, H., Kobayashi, H., West, A. R., Kanno, R. *et al., J. Electrochem. Soc.*, 2001, **148**, A730.
10. Kawai, H., Nagata, M., Tukamoto, H., Kageyama, H. and West, A. R., *Electrochim. Acta*, 1999, **45**, 315.
11. Gao, Y., Myrtle, K., Zhang, M., Reimers, J. N. and Dahn, J. R., *Phys. Rev. B*, 1996, **54**, 16670.
12. Zhong, Q., Banakdarpour, A., Zhang, M., Gao, Y. and Dahn, J. R., *J. Electrochem. Soc.*, 1997, **144**, 205.
13. Ein-Eli, Y. and Howard Jr., W. F., *J. Electrochem. Soc.*, 1997, **144**, L205.
14. Ein-Eli, Y., Howard Jr., W. F., Lu, S. H., Mukerjee, S., McBreen, J., Vaughey, J. T. *et al., J. Electrochem. Soc.*, 1998, **145**, 1238.
15. Fey, G. T.-K., Li, W. and Dahn, J. R., *J. Electrochem. Soc.*, 1994, **141**, 2279.
16. Van Landschoot, N., Kelder, E. M. and Schoonman, J., *Solid State Ionics*, 2004, **166**, 307.
17. Topas R Version 2.0, Bruker Analytical X-ray Software, 1999.
18. ASTM standard E902-88. *Surf. Interface Anal.* 1991, **17**, 889.
19. Moulder, J. F., Stickle, W. F., Sobol, P. E. and Bomben, K. B., *Handbook of X-ray Photoelectron Spectroscopy*. Perkin-Elmer, Wellesley, 1992.
20. Shirley, D. A., *Phys. Rev. B*, 1972, **5**, 4709.
21. Zview 2 Version 2.3d, Scribner Associates Inc., 1999.
22. Sickafus, K. E., Wills, J. M. and Grimes, N. W., *J. Am. Ceram. Soc.*, 1999, **82**(12), 3279.
23. NIST Standard Reference Database 20, Version 3.4 (Web Version, 2003), http://srdata.nist.gov/xps/, 2004.
24. Arrabito, M., Bodoardo, S., Penazzi, N., Panero, S., Reale, P., Scrosati, B. *et al., J. Power Sources*, 2001, **97–98**, 478.
25. Azad, A. K., Eriksson, S.-G., Yunus, S. M., Eriksen, J. and Rundlof, H., *Physica B*, 2003, **327**, 1.
26. Fey, G. T.-K., Lu, C.-Z. and Prem Kumar, T., *J. Power Sources*, 2001, **115**, 332.
27. Amine, K., Tukamoto, H., Yasuda, Y. and Fujita, Y., *J. Power Sources*, 1997, **68**, 604.
28. Fleisch, T. H. and Mains, G. J., *Appl. Surface Sci.*, 1982, **10**(1), 51.
29. Silversmit, G., Depla, D., Poelman, H., Marin, G. B. and De Gryse, R., *J. Electron Spectr. Rel. Phen.*, 2004, **135**, 167–175.
30. Hernan, L., Morales, J., Sanchez, L., Santos, J. and Rodriquez Castellon, E., *Solid State Ionics*, 2000, **133**, 179.
31. Jak, M. J. G., *Dynamic Compaction of Li-ion Battery Components and Batteries*. Ph.D Thesis, Delft University of Technology, 1999.
33. Molenda, J., Marzec, J., Świerczek, K., Ojczyk, W., Ziemnicki, M., Molenda, M. *et al., Solid State Ionics*, 2004, **171**(3/4), 215.
34. Marzec, J., Świerczek, K., PrzewoŹnik, J., Molenda, J., Simon, D. R. and Kelder, E. M., *J. Schoonman*, 2002, **146**(3/4), 225.